JOC The Journal of Organic Chemistry

Article

pubs.acs.org/joc

Mechanism of *N*-Hydroxylation Catalyzed by Flavin-Dependent Monooxygenases

Somayesadat Badieyan,*[,†] Robert D. Bach,[‡] and Pablo Sobrado*[,†,§]

[†]Department of Biochemistry, Virginia Tech, Blacksburg, Virginia 24061, United States

[‡]Departments of Chemistry and Biochemistry, University of Delaware, Newark, Delaware 19716, United States

[§]Virginia Tech Center for Drug Discovery, Virginia Tech, Blacksburg, Virginia 24061, United States

Supporting Information

ABSTRACT: *Aspergillus fumigatus* siderophore (SidA), a member of class B flavin-dependent monooxygenases, was selected as a model system to investigate the hydroxylation mechanism of heteroatom-containing molecules by this group of enzymes. SidA selectively hydroxylates ornithine to produce N^5-hydroxyornithine. However, SidA is also able to hydroxylate lysine with lower efficiency. In this study, the hydroxylation mechanism and substrate selectivity of SidA were systematically studied using DFT calculations. The data show that the hydroxylation reaction is initiated by homolytic cleavage of the O−O bond in the C^{4a}-hydroperoxyflavin intermediate, resulting in the formation of an internal hydrogen-bonded hydroxyl radical (HO•). As the HO• moves to the ornithine N^5 atom, it rotates and donates a hydrogen atom to form the C^{4a}-hydroxyflavin. Oxygen atom transfer yields an aminoxide, which is subsequently converted to hydroxylamine via water-mediated proton shuttling, with the water molecule originating from dehydration of the C^{4a}-hydroxyflavin. The selectivity of SidA for ornithine is predicted to be the result of the lower energy barrier for oxidation of ornithine relative to that of lysine (16 vs 24 kcal/mol, respectively), which is due to the weaker stabilizing hydrogen bond between the incipient HO• and O3′ of the ribose ring of $NADP^+$ in the transition state for lysine.

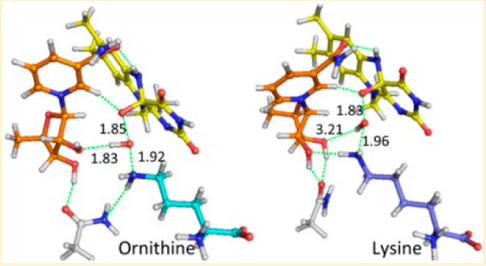

INTRODUCTION

Flavin-dependent monooxygenases are a large family of enzymes present in all kingdoms of life.[1] These enzymes are important in xenobiotic catabolism and the biosynthesis of sterols, fatty acids, and siderophores, among others.[2−4] On the basis of sequence similarity and structural features, flavoprotein monooxygenases are categorized into eight distinct classes (A through H).[5,6] Members of class B are able to hydroxylate both carbon atoms and heteroatoms, so they are called multifunctional flavoprotein monooxygenases and include flavin-containing monooxygenases (FMOs), Baeyer−Villiger monooxygenases (BVMOs), and *N*-hydroxylating monooxygenases (NMOs). In this class of enzymes, NADPH provides the reducing equivalents required for oxygen activation by the flavin cofactor. Furthermore, it has been shown that $NADP^+$ remains bound in the active site, where it plays an essential role in the stabilization of the hydroxylating species, the C^{4a}-(hydro)peroxyflavin (Scheme 1).[7−9]

NMOs are relatively less studied members of class B of flavin monooxygenases; however, these enzymes are pharmaceutically highly important.[10] NMOs are involved in *N*-hydroxylation of the long alkyl chain of primary amines such as lysine and ornithine.[5,11] The hydroxylated amines are subsequently incorporated into low-molecular-weight iron chelators known as siderophores.[12−14] Siderophore biosynthesis increases in response to iron shortages during infection in many bacterial and fungal pathogens.[15−17] The most studied NMOs are the ornithine hydroxylases from *Aspergillus fumigatus* (SidA)[18,19] and *Pseudomonas aeruginosa* (PvdA)[20,21] and the lysine hydroxylases from *Mycobacterium smegmatis* (MbsG) and *Escherichia coli* (IcuD).[22,23] Deletion of NMO genes in *A. fumigatus* and *P. aeruginosa* eliminates both siderophore synthesis and virulence, validating these enzymes as a target for drug development.[24−26] The mechanism of reaction by NMOs has been studied using kinetic and spectroscopic methods.[19,20,27,28] It has been shown that NMOs are highly selective for their amino acid substrates: lysine hydroxylases are able to hydroxylate only lysine, while ornithine hydroxylases are selective for ornithine.[19,29] Several high-quality crystal structures of SidA in different redox states and in complex with FAD, $NADP^+$, ornithine, and lysine make this enzyme an excellent model for computational studies. Here, quantum-mechanical (QM) methods were systematically applied to investigate the molecular mechanism of amino acid hydroxylation by SidA. Mainly the atomistic details of the reaction coordinates from the formation of the C^{4a}-hydroperoxyflavin−substrate complex to the production of the hydroxylated substrate and the selectivity of SidA for ornithine over lysine are described.

Received: November 20, 2014
Published: January 29, 2015

DOI: 10.1021/jo502651v
J. Org. Chem. 2015, 80, 2139−2147

Scheme 1. [a]

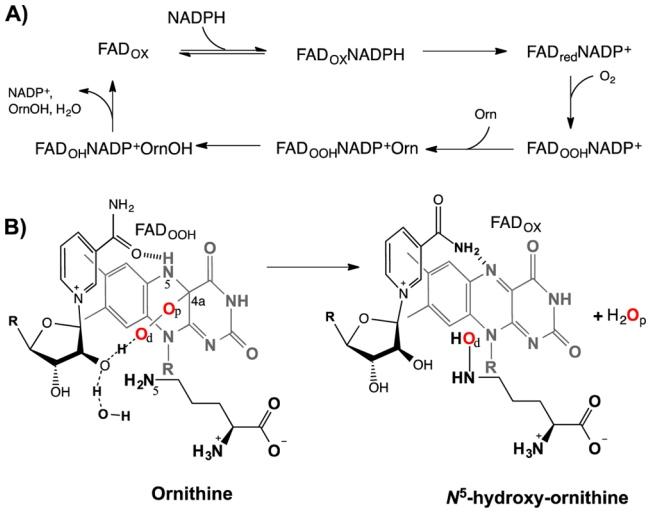

[a](A) Sequential kinetic mechanism for SidA. (B) Hydroxylation mechanism involving transfer of the distal oxygen (O_d) from the C^{4a}-hydroperoxyflavin–NADP$^+$–ornithine complex to the orn N^5 atom and ultimately the formation of hydroxylamine, which is the focus of this paper.

MATERIALS AND METHODS

DFT Analyses of the Model System. The structure of reduced SidA from *A. fumigatus* in complex with NADP$^+$ and ornithine (PDB entry 4B67)[18] was selected as the model system. Although the structure of oxidized SidA with bound lysine is available, the structure of this complex in the reduced form is not. To obtain coordinates for the SidA–lysine complex in the reduced state, the N^5 atom of ornithine in PDB entry 4B67 was replaced with $-CH_2-N^6$. To establish the proper hydrogen-bonding network, particularly for the SidA–lysine complex, the structures were subjected to restrained molecular dynamics (MD) simulations as previously described.[30] The minimal system to study the reaction mechanism quantum-mechanically included the catalytic molecules (FAD and Orn or Lys), NADP$^+$ (only the ribose and nicotinamide groups), and the residues within hydrogen-bonding distance from ornithine/lysine (Figure 1). The geometric coordinates of the C5′ atom of the ribose sugar in NADP$^+$, the C2′ atoms of the FAD model, and one carbon atom (preferably Cα) of each of the surrounding local residues were constrained as outlined in Figure 1.[30] This minimal level of atom constraint maintains the approximate X-ray distances between all of the components we included to describe the active site but still allows free motion of all of the interacting local atoms forming the key hydrogen bonds. The method of Polyak et al.[31] was used to add the peroxide group to reduced FAD.

The potential energy surfaces were scanned along the appropriate defined reaction coordinate using the B3LYP level of theory (default spin), with a 6-31G(d) basis set.[32] The resulting structures served as the starting point for subsequent geometry optimization, which was carried out using the same method with added diffuse functions. A larger basis set 6-311+G(p,d) was used for single point energy calculations on the optimized geometries.[33] All fully optimized geometries were followed by a complete frequency analysis to characterize the stationary points as either minima or first order saddle points. Based on the protonation state and type of substrate, the total number of atoms in each system varied from 150 to 155. All DFT calculations were conducted using the Gaussian 09 package.[34]

Energy Contributions by Active-Site Residues. The method offered by Tian et al.[35] was followed to calculate the energy contribution of each hydrogen-bond-making residue and NADP$^+$ during the hydroxylation reaction. In the optimized structures of reactants, transition states, and products, the residues were deleted one by one, and then B3LYP/6-311+G(d,p) single-point energy calculations were applied on each system without further optimization. The difference between the energy of the whole system (optimized structure with all residues) and the energy of that system minus the one residue was used to calculate the relative energy contribution (REC) of that residue.[36]

RESULTS AND DISCUSSION

The catalytic cycle of SidA has been characterized in detail.[8,19] The reaction is initiated by tight binding of NADPH to the oxidized enzyme, followed by stereospecific transfer of the *pro-R*-hydride equivalent to the flavin cofactor.[8] The reduced flavin reacts with molecular oxygen to ultimately form the C^{4a}-hydroperoxyflavin (FAD_{OOH}), which is the hydroxylating species (Scheme 1). The formation of this hydroperoxy intermediate is accelerated by binding of ornithine, lysine, and arginine.[18,19] However, SidA is >10-fold more selective for ornithine over lysine and does not hydroxylate arginine.[30] The mechanism of hydroxylation in SidA has not been probed by any biochemical or computational methods. Conventional

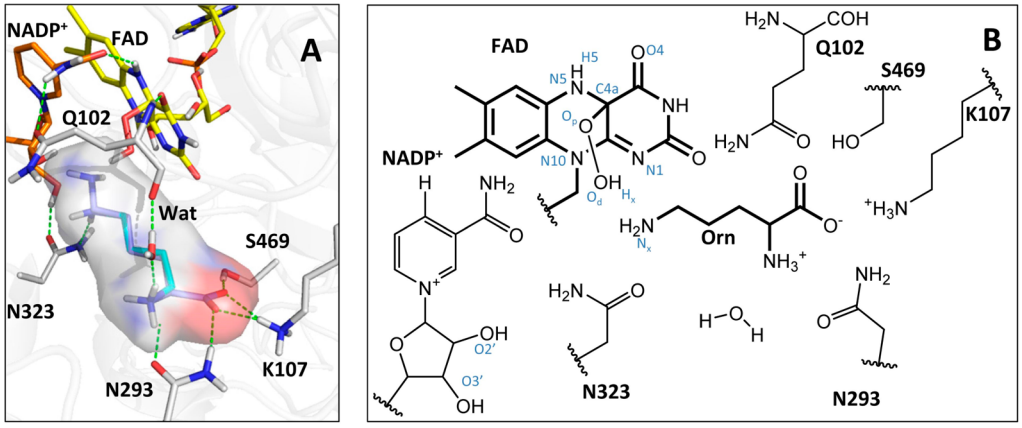

Figure 1. (A) Hydrogen-bonding interactions in the active site of SidA (PDB entry 4B67). FAD, NADP$^+$, ornithine, and lysine are shown in yellow, orange, cyan, and purple carbons, respectively. (B) Fragments of FAD, NADP$^+$, and interacting residues that were included in the DFT calculations for the *N*-hydroxylation reaction by SidA. With the exception of Q102, only the side chains of the other residues were considered for the QM study. The points of positional restraint are illustrated with squiggle lines. At the B3LYP/6-31G(d) level, this included 1526 basis functions. For the hydroxylation of Lys, the amine group of ornithine was replaced with $-CH_2-NH_2$ (1549 basis functions).

DOI: 10.1021/jo502651v
J. Org. Chem. 2015, 80, 2139–2147

wisdom suggests that the hydroxylation process occurs via nucleophilic attack of the side-chain N^x group on the distal oxygen (O_d) of FAD_{OOH}, a mechanism generally thought to occur in other flavin-dependent hydroxylation reactions.[37−41] In this work, DFT calculations on the SidA complexes were performed to gain insight into the mechanism of hydroxylation. Furthermore, taking advantage of the availability of the structure of SidA in complex with $NADP^+$ and lysine, we explored the mechanism of substrate selectivity. We present theoretical data suggesting that the mechanism of FAD_{OOH} oxidation proceeds by substrate-initiated homolytic cleavage of the O−O bond that produces an internally bound $HO^\bullet$ radical as the primary oxidant.

Protonation of the Ground-State SidA−Substrate Complex. Activation of molecular oxygen by reduced flavin occurs via a single-electron-transfer step that yields a flavin semiquinone and an superoxide anion.[42,43] This radical pair is believed to collapse, forming the C^{4a}-peroxyflavin intermediate (FAD_{OO^-}).[42,43] The catalytically competent intermediate in the hydroxylation reaction is the protonated form of this intermediate, FAD_{OOH} (Scheme 1).[43,44] Using stopped-flow time-resolved spectroscopy analyses, solvent kinetic isotope effects, and DFT calculations, we showed that FAD_{OOH} is formed via a proton transfer to the FAD_{OO^-} mediated by the 2′-OH of the nicotinamide ribose of $NADP^+$ and proved that ornithine binds with the N^5 atom in its neutral form ($-NH_2$).[30] To explore the ground-state SidA−Lys complex, the hydrogen-bonding network of the flavin intermediate was also investigated with lysine bound in the active site using the B3LYP/6-31+G(d) method, and these results were compared with those obtained in the presence of ornithine. The system was studied with FAD_{OO^-}, or FAD_{OOH}, in complex with lysine having its N^6 atom in the neutral form. In the energy-optimized geometry of the FAD_{OO^-}−Lys complex, a hydrogen bond between the peroxide moiety and the ribose 2′-OH (observed with ornithine) is interrupted when lysine is bound; consequently, the only hydrogen-bond donor to the anionic O_d is the lysine N^6H moiety (Figure S1D in the Supporting Information). As observed with the FAD_{OO^-}−Orn complex, the nicotinamide group is hydrogen-bonded to O_d instead of the proximal oxygen (O_p), and the interaction between the carbonyl of the $NADP^+$ amide and the hydrogen of the FAD-N^5 atom is lost in this complex (Figure S1D and ref 30). This interaction has been shown to be essential for stabilization of FAD_{OOH} in SidA and other flavin monooxygenases. These results indicate that FAD_{OO^-} is not predicted to be stable when Lys is bound, consistent with the previous results obtained with Orn.[30]

Analysis of the FAD_{OOH}−Lys and −Orn complexes showed two hydrogen-bonding orientations: FAD_{OOH} acting as hydrogen-bond donor and the amine group of Orn/Lys as a hydrogen-bond acceptor and vice versa (Figure S1). If O_d of FAD_{OOH} acts as the hydrogen-bond acceptor with N^xH_2 of Lys/Orn as the donor, it makes a weak hydrogen bond as a donor to the ribose 3′-OH of the ribose ring. This complex is always less stable than the complex in which HO_d functions as a hydrogen-bond donor, where the hydrogen bond made by HO_d to N^x of the substrate is in the range of ∼1.7 Å ($H\cdots N^x$ distance in the Lys or Orn complex) (Figure S1C,F). The differences between the energies of these two hydrogen-bonding patterns are 2.12 and 4.21 kcal/mol for the FAD_{OOH}−Orn and FAD_{OOH}−Lys complexes, respectively.

These combined results are consistent with previous studies[30,40] suggesting that the primary hydrogen-bonding interaction in FADOOH−Orn/Lys complexes involves the interaction of the more acidic OOH proton with the more basic NH_2 nitrogen lone pair.

Oxygen Transfer from FAD_{OOH}. To explore the reaction pathway, a potential energy scan was performed starting from the optimized FAD_{OOH}−Orn (Figure S1C) or FAD_{OOH}−Lys (Figure S1F) reactant complex (Figure 2). The reaction

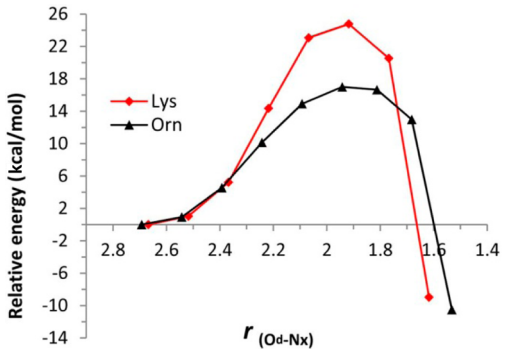

Figure 2. Potential energy surfaces for the oxidations of Lys and Orn by SidA. For each complex, the reaction coordinate was defined as the distance between the distal oxygen of the C^{4a}- hydroperoxyflavin (O_d) and the N^x atom of the amino acid ligand at the B3LYP/6-31G(d) level of theory.

coordinate was defined as the distance between HO_d (the protonated distal oxygen) of FAD_{OOH} and the N^x atom of the amino acid substrate. During the simulation, this distance was sequentially decreased from 2.7 Å in several steps of 0.15 Å until a value of ∼1.5 Å was reached. The resulting potential energy curves were relatively smooth until the saddle point (at a distance close to 1.9 Å), with maxima of about 16 and 24 kcal/mol for Orn and Lys, respectively. Starting with the calculated coordinates at the maximum points in the energy profiles, the energy-optimized geometries of the TSs were obtained as depicted in Figure 3B,B′, while the coordinates of a single carbon atom of each local residue were constrained in order to maintain the general juxtaposition of the residues in the X-ray structure (Figure 1B). No geometry constraints were placed upon the substrate (Orn or Lys) so it could move about in the local pocket during the oxidation step. The results show that during the oxygen atom transfer step for the Orn oxidation, the HO group being transferred is suspended nearly equidistant between the proximal oxygen ($r_{(O_p-O_d)}$ = 1.84 Å) and the N^x atom ($r_{(O_p-N^x)}$ = 1.94 Å).

The net charge on the transferring HO_d group in both transition states was found to be essentially zero (Table 1). A natural bond order (NBO) analysis[45] suggested that the $HO^\bullet$ radical fragment in the Orn TS (Figure 3B) had a charge of only −0.02*e*, while in the Lys TS (Figure 3B′) that charge was −0.04*e*. Additionally, frequency calculations for this type of TS show that the oxygen of the HO_d group oscillates back and forth between the oxygen and nitrogen in a windshield-wiper motion, while there is little or no motion of the H atom of the HO_d group. Also, there is essentially no movement of the Lys/Orn N^x or the leaving FAD O_p group. It has been demonstrated that when largely heavy-atom motion (oxygen) is involved in the TS, then the magnitude of the imaginary frequency is typically quite small (less than 400 cm^{-1}), while involvement of

DOI: 10.1021/jo502651v
J. Org. Chem. 2015, 80, 2139−2147

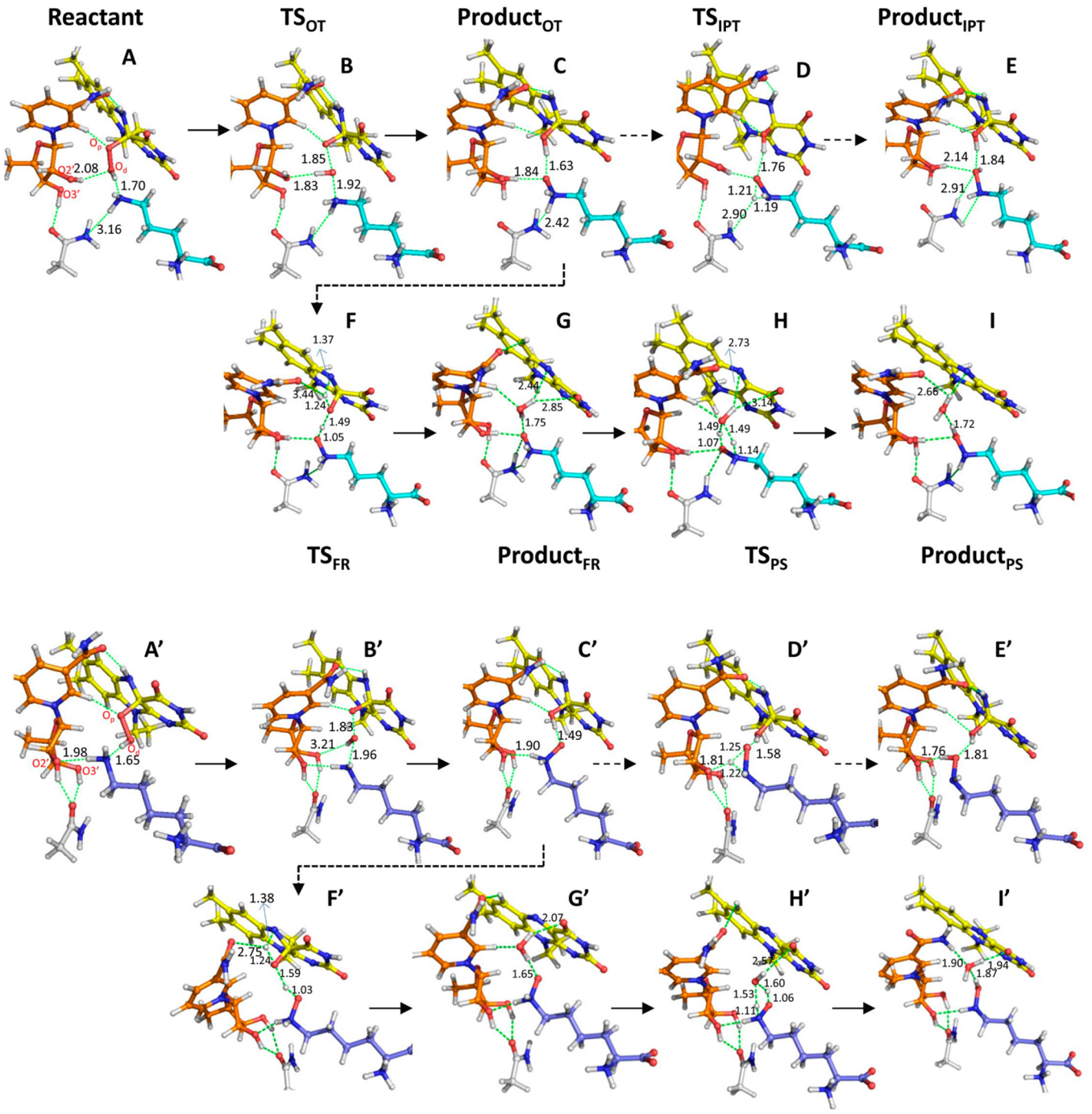

Figure 3. B3LYP/6-31+G(d) geometry-optimized structures along the hydroxylation reactions of (A–I) ornithine and (A′–I′) lysine. The four studied steps are oxygen transfer (OT) as a hydroxyl radical group (HO$^{\bullet}$), intermolecular proton transfer (IPT) from N^{x} to the oxygen atom on the aminoxide, oxidized flavin regeneration (FR) by dehydration of FAD$_{OH}$, and proton shuttling (PS) mediated by the released water molecule. The lengths (in Å) of all hydrogen bonds shown are measured as the distance between the hydrogen and the accepting heavy atom.

mostly light-atom motion (hydrogen) is associated with an imaginary frequency of magnitude approaching 1000 cm^{-1} or more.[41] Upon identifying the imaginary frequency associated with the oxygen atom transfer in the Orn TS, we observed it to have a magnitude of 370 cm^{-1}, while that for the Lys TS was 341 cm^{-1}. These data are clearly consistent with the concept that movement in the TS consists largely of motion of the oxygen atom of the HO$^{\bullet}$ radical.

This observation is consistent with earlier reports where this oxidative step was attributed to a somersault-like rearrangement of FAD$_{OOH}$ (FAD$_{O-OH}$ → FAD$_{O\cdots HO}$) that produces an internally hydrogen-bonded HO$^{\bullet}$ radical in which the O···O···N^{x} moiety in the TS is essentially linear and the H atom of the HO$_{d}$ group is perpendicular to this axis and hydrogen-bonded to the proximal oxygen ($r_{(H_x-O_p)}$ = 1.99 Å) and the ribose O2′ oxygen, as noted in Orn TS$_{OT}$ (Figure 3B). The classical activation barrier for this homolytic O–O bond cleavage is 27.0 kcal/mol in the absence of a substrate, supporting the suggestion that this rearrangement is induced by complexation of the OOH moiety of the hydroperoxide to the

DOI: 10.1021/jo502651v
J. Org. Chem. 2015, 80, 2139–2147

Table 1. Critical Distances (in Å) and Mulliken Charges (in au) for Each Complex along the Hydroxylation Reaction of Ornithine and Lysine after Geometry Optimization[a]

		distances			charges			
amino acid	structure	C4(FAD)−O_d	O_d−O_p	O_p−N^x	O_d	O_p	H_x	N^x
Orn	Reactant	1.501	1.455	2.627	−0.321	−0.484	0.487	−0.794
	TS_{OT}	1.389	1.849	1.919	−0.537	−0.441	0.453	−0.601
	$Product_{OT}$	1.432	2.64	1.395	−0.682	−0.615	0.451	−0.329
	TS_{IPT}	1.442	2.732	1.528	−0.639	−0.63	0.46	−0.489
	$Product_{IPT}$	1.447	2.803	1.458	−0.663	−0.566	0.454	−0.362
	TS_{FR}	1.426	2.539	1.409	−0.725	−0.548	0.484	−0.356
	$Product_{FR}$	3.400	2.701	1.396	−0.854	−0.578	0.422	−0.336
	TS_{PS}	3.501	2.436	1.425	−0.904	−0.545	0.441	−0.405
	$Product_{PS}$	3.500	2.708	1.453	−0.848	−0.610	0.469	−0.388
Lys	Reactant	1.469	1.464	2.645	−0.328	−0.492	0.485	−0.835
	TS_{OT}	1.398	1.823	1.960	−0.515	−0.444	0.447	−0.661
	$Product_{OT}$	1.425	2.526	1.389	−0.682	−0.604	0.466	−0.351
	TS_{IPT}	1.435	2.644	1.510	−0.662	−0.627	0.475	−0.494
	$Product_{IPT}$	1.443	2.690	1.455	−0.65	−0.618	0.463	−0.395
	TS_{FR}	1.456	2.562	1.407	−0.720	−0.538	0.446	−0.394
	$Product_{FR}$	3.403	2.660	1.391	−0.889	−0.627	0.438	−0.356
	TS_{PS}	3.074	2.510	1.425	−0.924	−0.556	0.444	−0.435
	$Product_{PS}$	3.261	2.846	1.460	−0.867	−0.630	0.450	−0.409

[a]The geometry optimizations were performed at the B3LYP/6-31+G(d) level of theory. The subscripts refer to different steps of the reaction: OT for oxygen transfer, IPT for intermolecular proton transfer, FR for flavin regeneration, and PS for proton shuttling.

substrate NH_2 group because the barrier for O−O bond cleavage attending the *N*-oxidation of Orn is only 16 kcal/mol.[46,47] It is also noted that in the TS the HO• radical is strongly hydrogen-bonded to the 2′-oxygen of the $NADP^+$ ribose moiety ($r_{(H_x-O2')}$ = 1.83 Å). It is essential that the reactivity of this internally bound HO• radical be tempered by such hydrogen-bonding interactions because it can abstract H atoms indiscriminately in the absence of this stabilizing influence. In fact, it is very likely that this strong hydrogen bond to the adjacent 2′-oxygen is largely responsible for the lower activation barrier for Orn oxidation relative to Lys oxidation ($\Delta\Delta E^{\ddagger}$ = 8 kcal/mol). The TS coordination was slightly different between Orn and Lys, as in the TS of the FAD_{OOH}−Lys complex HO_d makes a weak hydrogen bond to O3′ of ribose ($r_{(H_x-O3')}$ = 3.21 Å) because the N^x atom of Lys is already donating a hydrogen bond to ribose's 2′-OH. The critical distances are almost the same for the two complexes in the transition state: $r_{(O_p-O_d)}$ is 1.84 ± 0.01 Å and $r_{(O_p-N)}$ is 1.94 ± 0.02 Å (averaged over the equivalent values for Orn and Lys complexes). Therefore, the increase of ∼8 kcal/mol in the energy barrier for oxidation of Lys relative to Orn can be attributed to the different orientation of the HO• radical (due to the spatial restraint of the SidA active site in each reactant complex) and the much stronger hydrogen-bonding interaction of the HO• to the 2′-OH group (1.829 Å) in the transition state of Orn relative to that for Lys binding (3.21 Å to O3′).

When $r_{(O_d-N)}$ reaches ∼1.7 Å, the atoms at the center of the reaction rearrange, and the hydroxyl radical loses its hydrogen bond to the ribose 2′-OH and faces toward the FAD $O_p^{\bullet}$ radical, followed by a rapid hydrogen transfer from the $HO_d^{\bullet}$ group to the FAD $O_p^{\bullet}$ radical to form FAD_{OH} late along this concerted pathway (Figure 3C,C′). The steep change in the potential energy surface at $r_{(O_d-N)} \approx 1.7$ Å is coupled to this rearrangement. At the end of this step, the ribose O2′ that was hydrogen-bonded to the HO• radical in the TS reorients to donate a hydrogen bond to O_d (now part of the oxygenated amino acid; Figure 3C,C′). These data provide additional support for the "somersault rearrangement" mechanism that has also been proposed for FMO and P450 monooxygenases.[46,47] The results for SidA further support a new mechanism that is different from the accepted nucleophilic displacement (S_N2) by the sp^3-hybridized nitrogen to HO_d of FAD_{OOH}.[37−41] In summation, the product of this initial step is predominantly a primary alkyl amine *N*-oxide, retaining its two hydrogen atoms on the amine nitrogen. In this kinetic product, $r_{(O_d-N)}$ is >0.05 Å shorter than this length in the energy-optimized geometry of the N^5-hydroxyornithine (Table 1), and the charge distribution on the produced aminoxide (Table 1) indicates that the negative charge on O_d is now increased by average of 0.35*e* while that on N^x is decreased by 0.47*e*.

Formation of Hydroxylamine. *Intramolecular Proton Transfer.* Upon formation of an alkyl aminoxide in the penultimate oxygen atom transfer reaction, the final product is formed by protonation of the transferred oxygen (O_d) and deprotonation of the nitrogen (N^x). Structural analyses of the active site of SidA in the presence of Lys/Orn show that no space is available for a water molecule to be accommodated close to the aminoxide to mediate the protonation/deprotonation reaction.[30] Taking this structural constraint into account, three scenarios for proton transfer can be considered: (1) protonation occurs via an intramolecular proton transfer from the N^x atom, a mechanism previously proposed on the basis of computational studies for hydroxylation of primary amines by cytochrome P450s;[48] (2) dehydration of FAD_{OH} occurs in the presence of the alkyl aminoxide, and the resulting water molecule facilitates the proton shuttle; or (3) the primary aminoxide, ornithine N^5-oxide, is the final product of the enzymatic reaction, and protonation/deprotonation happens nonenzymatically in solution after this molecule is released. To ascertain whether an intramolecular proton transfer occurs in

DOI: 10.1021/jo502651v
J. Org. Chem. 2015, 80, 2139−2147

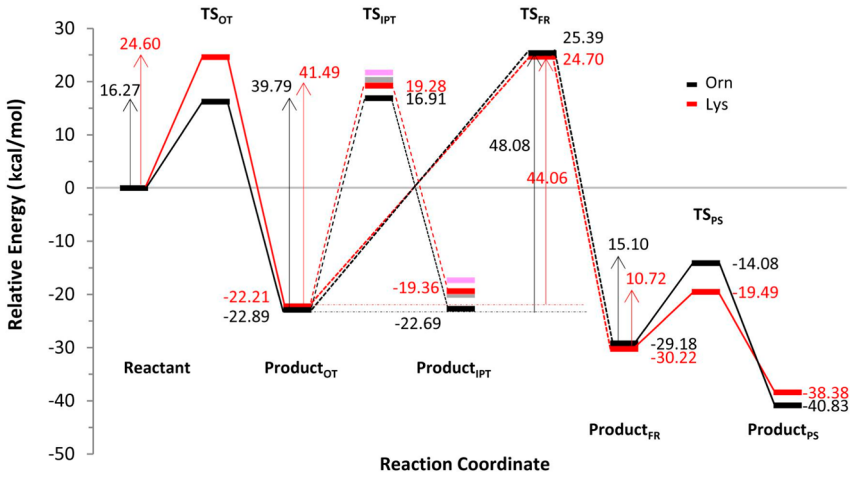

Figure 4. Relative energy profiles for the hydroxylation reactions of Orn and Lys catalyzed by SidA, calculated at the B3LYP/6-311+G(d,p) level. The steps of the reaction are denoted as OT for oxygen transfer, IPT for intermolecular proton transfer, FR for flavin regeneration, and PS for proton shuttling. The gray and pink bars refer to the less favorable proton transfer (out of two) in the intramolecular proton transfer step in the Orn and Lys complex, respectively.

SidA, the activation energies required for the transfer of either of the two hydrogens on N^x to the oxygen atom were calculated. The relative energy values for the two hydrogens do not differ significantly (the differences in the energy barriers are 3.4 and 2.5 kcal/mol for the ornithine and lysine complexes, respectively; Figure 4). Interestingly, this step is endothermic, and the enzyme−FAD_{OH}−hydroxylamine complex is energetically less favorable than the enzyme−FAD_{OH}−amine oxide product complex (Figure 4).

Although the energies of reaction for the intramolecular proton rearrangement steps are only +0.2 and +2.85 kcal/mol for Orn and Lys, respectively, the considerably large activation energies for this step (39.79 and 41.49 kcal/mol for Orn and Lys, respectively; Figure 4) exclude any equilibration assumption. On the basis of these results, it can be concluded that the aminoxide form of ornithine/lysine is the final product of the enzymatic reaction and that the proton rearrangement most likely occurs upon release of the amine oxide product to the bulk solution. Alternatively, the formation of the hydroxyornithine/lysine could happen via the second scenario (see the next section).

Water-Mediated Proton Transfer. The decay of C^{4a}-hydroxyflavin (FAD_{OH}) to regenerate the oxidized flavin occurs with the release of the oxygenated product and water from the active site (Scheme 1). In most flavin monooxygenases, these two steps are not distinguishable in kinetic experiments[49] and FAD_{OH} eliminates water either prior to or concomitant with product release.[50,51] FAD_{OH} dehydration is proposed to occur by hydrogen transfer from the FAD N^5−H to the hydroxyl group (O_pH).[30,52,53] If the dehydration reaction occurs before product release, we wondered whether the eliminated water molecule could assist in the proton transfer in the aminoxide. To answer this question, we studied the dehydration of FAD_{OH} by direct transfer of the N^5 hydrogen to the OH group of FAD_{OH} in the presence of ornithine (lysine) oxide. In the absence of any acid/base to assist the hydrogen transfer, this step needs to overcome high energy barriers of 48.08 and 44.06 kcal/mol for the ornithine and lysine complexes, respectively (Figure 4, TS_{FR}). The products of this step (aminoxide + water + FAD) are 6−8 kcal/mol lower in energy than the complex of aminoxide and FAD_{OH} (Figure 4, $Product_{FR}$). The released water molecule maintains its hydrogen bond to the oxygen of the aminoxide while it weakly donates hydrogen bonds to the FAD N^5 and the FAD O_4. The observed orientation of the water molecule in the active site supports its role as a proton shuttle in the formation of a hydroxylamine from the related aminoxide (Figure 3G,G′). In the next step, the potential energy surface was scanned along with the decrease in the distance between the oxygen of the water molecule and the hydrogen on N^x of Lys or Orn. From the two hydrogen atoms on N^x, the one that was at a shorter distance to the water oxygen was selected to define the reaction coordinate, and scanning was stopped when $r_{(O_p-N^x)}$ reached 1 Å. The activation energies required for water-mediated proton transfer on the aminoxide were found to be as low as 15.10 and 10.72 kcal/mol for ornithine oxide and lysine oxide, respectively, in the active site of SidA (Figure 4, TS_{PS}). The lower energy barrier for Lys oxide can be related to the retention of the hydrogen bond made by water to the FAD O_4 at the transition state (Figure 3H′). The final products of this step (HO-Lys/HO-Orn + water + FAD) are 11.65 and 8.16 kcal/mol more stable than the reactants (aminoxide + water + FAD_{OH}) for the Orn and Lys complexes, respectively (Figure 4, $Product_{PS}$). In the optimized geometry of the product, the regenerated water from the proton shuttling reaction orients and interrupts the hydrogen bond between the nicotinamide moiety of $NADP^+$ and the side chain of Q102, which may initiate the release of $NADP^+$ from the active site (Figure 3I,I′). The energies of the final products are 38.38 and 40.83 kcal/mol lower than those for the starting enzyme−ligand combinations (Orn/Lys + FAD_{OOH}) (Figure 4, $Product_{PS}$). Since the overall reactions are highly exothermic for both substrates via this pathway, a hydroxylated amino acid is more likely to be the final product of the enzymatic reaction. However, SidA needs to overcome the relatively high energy barrier for dehydration of FAD_{OH}. Recently it was shown that proton shuttle mediators are required in order to lower the activation energy for elimination of H_2O_2 from FAD_{OOH}.[54] It is reasonable to assume that some local conformational adjustments may occur upon the formation of the aminoxide that relocate the active-site residues (e.g., Arg144) and water molecules in the vicinity of the FAD N^5−H. The relocated groups may function as hydrogen-bond

DOI: 10.1021/jo502651v
J. Org. Chem. 2015, 80, 2139−2147

mediators that facilitate the dehydration reaction and lower its energy barrier in SidA.

The Role of Active-Site Residues and NADP$^+$ in Catalysis. To determine the role of residues in the active site of SidA and NADP$^+$ on the energy profile of the *N*-oxidation reaction, side chains of all residues that are hydrogen-bonded to Orn and NADP$^+$ (ribose + nicotinamide ring) were treated one by one using DFT/B3LYP calculations as described in Materials and Methods. Results from the REC calculations are shown in Figure 5. NADP$^+$ plays a major role in the energy profile and energetically contributes more to the stabilization of the amine oxide products than the TSs. The O2′ hydroxyl group on the ribose moiety of NADP$^+$ is expected to be the central atom in this energy contribution by the formation of a hydrogen bond to the aminoxide product (oxygen in the ornithine oxide and nitrogen in the lysine oxide). Q102, which is conserved among SidA, PvdA, and IcuD, forms a hydrogen bond to the FAD O_4 atom. Additionally, a water molecule is hydrogen-bonded between Q102 and the α-amino group of the amino acid substrate. Because of the long and flexible side chain of this residue, it contributes differently at each step of the oxidation reaction. In reference to the enzyme−reactant complex, it makes its maximum energy contribution in the product of the lysine oxidation step, which stabilizes the transferred O_d by extending its hydrogen bond from O_4 of FAD to O_d in the oxidized lysine.

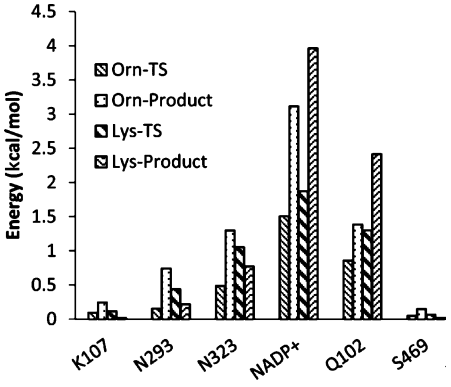

Figure 5. Relative energy contributions (RECs) of the active-site residues and NADP$^+$ to the oxidation step of the *N*-hydroxylation reaction catalyzed by SidA. The reference for the calculation of REC values is the optimized reactant of the enzyme−substrate complex (Orn or Lys). REC values were calculated at the B3LYP/6-311+G(d,p) level.

Although N323 makes a direct hydrogen bond to the Orn N^5 atom in all of the steps of ornithine oxidation, its contribution to the energy profile does not change significantly from the reference geometry (enzyme−reactant complex) because its orientation remains almost unchanged along the reaction coordinate. The residue equivalent to this asparagine in *E. coli* lysine hydroxylase (IcuD) is a serine.[11] The smaller residue may provide extra space for IcuD to accommodate lysine in front of FAD_{OOH} in a way that allows the $HO_d^\bullet$ radical being transferred to interact with O2′ of NADP$^+$ instead of O3′ in the transition state (as happens in the oxidation of lysine by SidA). The other residues that interact with the α-amino or carboxyl groups of Orn/Lys (K107, N293, and S469) show small REC values in the energy profile, as they interact with the α-groups of the amino acid substrates and their orientation is not affected during the oxidation reaction.

Scheme 2. Proposed Mechanism for the *N*-Hydroxylation of Primary Amines by SidA Demonstrating the Windshield-Wiper Motion of the HO$^\bullet$ Oxygen in Concert with H-Atom Migration[a]

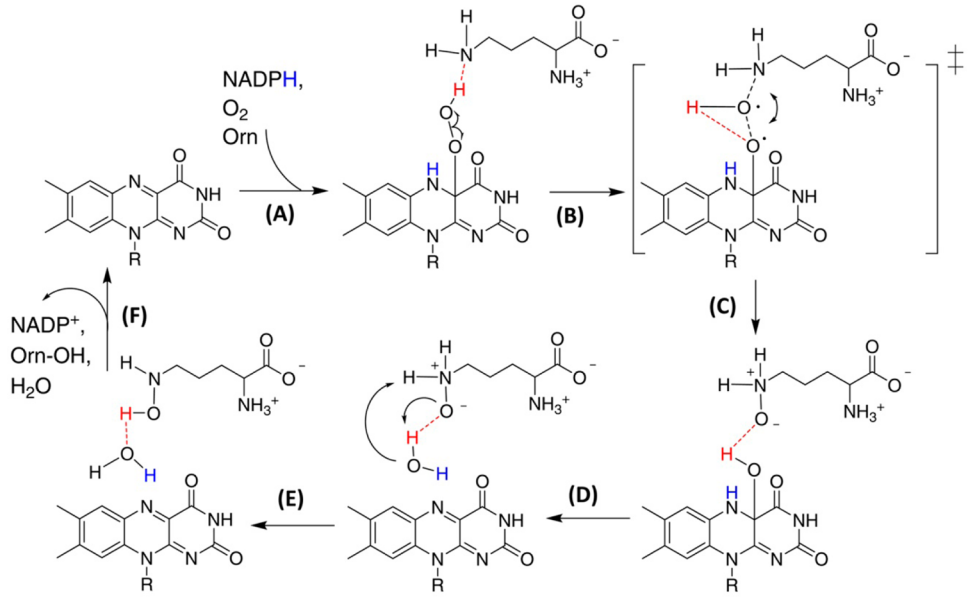

[a]The ornithine substrate induces hemolytic cleavage of the O−OH bond in C^{4a}-hydroperoxyflavin (B). Transfer of the HO$^\bullet$ radical occurs via a somersault rearrangement, which allows the transfer of the H atom from the $^\bullet$OH to the $FAD_{O\bullet}$ to form FAD_{OH} and the Orn aminoxide (C). Water released from FAD_{OH} catalyzes the deprotonation/protonation steps to form the final HO-Orn (E, D). The final step is the release of products (F). It should be noted that NADP$^+$ remains bound in the active site but has been omitted here for clarity. The red dashed lines show the hydrogen bonds.

DOI: 10.1021/jo502651v
J. Org. Chem. 2015, 80, 2139−2147

CONCLUSIONS

We have described the details of the hydroxylation mechanism and substrate selectivity in the reaction catalyzed by flavin-dependent *N*-hydroxylating monooxygenases. Analysis of the energy profiles along the reaction coordinates starting from the geometry-optimized FAD_{OOH}−Orn/Lys complexes show that the chemical events in this enzymatic reaction are initiated by a homolytic O−O bond cleavage induced by complexation of FAD_{OOH} with the substrate. This step has been described previously as a somersault rearrangement ($FAD_{O-OH} \rightarrow FAD_{O\cdots HO}$) of the intermediate hydroperoxide to the $FAD_{O}^{\bullet}$ radical, producing an internally hydrogen-bonded $HO^{\bullet}$ radical as the primary oxidant. In the present study, complexation of FAD_{OOH} with the substrate NH_2 group initiates a homolytic O−O bond rupture in concert with a partial rearrangement of the OOH group and production of an internally hydrogen bonded $HO^{\bullet}$ radical with an accompanying one-step oxygen transfer from FAD_{OOH} to the nitrogen atom (Scheme 2).

In the transition state, the radical group ($HO^{\bullet}$) is stabilized by hydrogen bonding to O2′ or O3′ of the ribose moiety of $NADP^{+}$ in the ornithine and lysine complexes, respectively. This variation in the hydrogen bonding of the $HO^{\bullet}$ group results in a higher energy barrier for the oxidation of lysine (24 vs 16 kcal/mol), which is partially responsible for the observed selectivity of SidA for Orn versus Lys.[30] This somersault-type rearrangement leads to transfer of the hydrogen atom from the $HO^{\bullet}$ group to the flavin oxyradical and the formation of an *N*-alkyl aminoxide. The aminoxide may be considered the final product of the enzymatic reaction if the decay of FAD_{OH} occurs after product release. In this case, the proton exchange to generate the hydroxylamine may happen later in the interaction of the product of the oxidation step with the bulk solvent. If dehydration of FAD_{OH} occurs prior to release of the product, it provides the water molecule that shuttles the proton transfer on the *N*-alkyl aminoxide to form the final hydroxy amino acid. Here, the final products (hydroxylamine + water + oxidized FAD) are 38.38 and 40.83 kcal/mol more stable than the initial reactants (Orn/Lys + $FADO_{OH}$) for Orn and Lys, respectively. Since the total reaction energies are highly favorable for both substrates in the latter pathway, hydroxylamine is more likely the final product of the reaction of SidA.

ASSOCIATED CONTENT

Supporting Information

Optimized prereaction structures of SidA in complex with Lys and Orn in different protonation states and *XYZ* coordinates of optimized geometry for each Orn/Lys complex (core of reactions). This material is available free of charge via the Internet at http://pubs.acs.org.

AUTHOR INFORMATION

Corresponding Authors

*E-mail: badieyan@vt.edu (S.B.).
*E-mail: psobrado@vt.edu (P.S.).

Notes

The authors declare no competing financial interest.

ACKNOWLEDGMENTS

This work was supported by a grant from the National Science Foundation (MCB-1021384). We thank the Virginia Tech Computing Facility for computing time on the BlueRidge and HokieOne supercomputers. We are also grateful to GridChem for computational resources (www.gridchem.org).

REFERENCES

(1) Huijbers, M. M.; Montersino, S.; Westphal, A. H.; Tischler, D.; van Berkel, W. J. *Arch. Biochem. Biophys.* **2014**, *544*, 2.
(2) Laden, B. P.; Tang, Y. Z.; Porter, T. D. *Arch. Biochem. Biophys.* **2000**, *374*, 381.
(3) Schlaich, N. L. *Trends Plant Sci.* **2007**, *12*, 412.
(4) Crosa, J. H.; Walsh, C. T. *Microbiol. Mol. Biol. Rev.* **2002**, *66*, 223.
(5) van Berkel, W. J.; Kamerbeek, N. M.; Fraaije, M. W. *J. Biotechnol.* **2006**, *124*, 670.
(6) Pazmino, D. E. T.; Winkler, M.; Glieder, A.; Fraaije, M. W. *J. Biotechnol.* **2010**, *146*, 9.
(7) Alfieri, A.; Malito, E.; Orru, R.; Fraaije, M. W.; Mattevi, A. *Proc. Natl. Acad. Sci. U.S.A.* **2008**, *105*, 6572.
(8) Romero, E.; Fedkenheuer, M.; Chocklett, S. W.; Qi, J.; Oppenheimer, M.; Sobrado, P. *Biochim. Biophys. Acta* **2012**, *1824*, 850.
(9) Orru, R.; Dudek, H. M.; Martinoli, C.; Torres Pazmino, D. E.; Royant, A.; Weik, M.; Fraaije, M. W.; Mattevi, A. *J. Biol. Chem.* **2011**, *286*, 29284.
(10) Badieyan, S.; Sobrado, P. In *Microbial Pathogens and Strategies for Combating Them: Science, Technology and Education*; Mendez-Vilas, A., Ed.; Formatex Research Center: Badajoz, Spain, 2013; p 430.
(11) Olucha, J.; Lamb, A. L. *Bioorg. Chem.* **2011**, *39*, 171.
(12) Neilands, J. B. *J. Biol. Chem.* **1995**, *270*, 26723.
(13) Hider, R. C.; Kong, X. *Nat. Prod. Rep.* **2010**, *27*, 637.
(14) Haas, H.; Eisendle, M.; Turgeon, B. G. *Annu. Rev. Phytopathol.* **2008**, *46*, 149.
(15) Weinberg, E. D. *Biochim. Biophys. Acta* **2009**, *1790*, 600.
(16) Abergel, R. J.; Wilson, M. K.; Arceneaux, J. E. L.; Hoette, T. M.; Strong, R. K.; Byers, B. R.; Raymond, K. N. *Proc. Natl. Acad. Sci. U.S.A.* **2006**, *103*, 18499.
(17) Fischbach, M. A.; Lin, H.; Liu, D. R.; Walsh, C. T. *Nat. Chem. Biol.* **2006**, *2*, 132.
(18) Franceschini, S.; Fedkenheuer, M.; Vogelaar, N. J.; Robinson, H. H.; Sobrado, P.; Mattevi, A. *Biochemistry* **2012**, *51*, 7043.
(19) Chocklett, S. W.; Sobrado, P. *Biochemistry* **2010**, *49*, 6777.
(20) Meneely, K. M.; Lamb, A. L. *Biochemistry* **2007**, *46*, 11930.
(21) Olucha, J.; Meneely, K. M.; Chilton, A. S.; Lamb, A. L. *J. Biol. Chem.* **2011**, *286*, 31789.
(22) Thariath, A.; Socha, D.; Valvano, M. A.; Viswanatha, T. *J. Bacteriol.* **1993**, *175*, 589.
(23) Thariath, A. M.; Fatum, K. L.; Valvano, M. A.; Viswanatha, T. *Biochim. Biophys. Acta* **1993**, *1203*, 27.
(24) Hissen, A. H. T.; Wan, A. N. C.; Warwas, M. L.; Pinto, L. J.; Moore, M. M. *Infect. Immun.* **2005**, *73*, 5493.
(25) Sokol, P. A.; Darling, P.; Woods, D. E.; Mahenthiralingam, E.; Kooi, C. *Infect. Immun.* **1999**, *67*, 4443.
(26) Takase, H.; Nitanai, H.; Hoshino, K.; Otani, T. *Infect. Immun.* **2000**, *68*, 1834.
(27) Meneely, K. M.; Barr, E. W.; Bollinger, J. M., Jr.; Lamb, A. L. *Biochemistry* **2009**, *48*, 4371.
(28) Mayfield, J. A.; Frederick, R. E.; Streit, B. R.; Wencewicz, T. A.; Ballou, D. P.; DuBois, J. L. *J. Biol. Chem.* **2010**, *285*, 30375.
(29) Frederick, R. E.; Mayfield, J. A.; DuBois, J. L. *J. Am. Chem. Soc.* **2011**, *133*, 12338.
(30) Robinson, R.; Badieyan, S.; Sobrado, P. *Biochemistry* **2013**, *52*, 9089.
(31) Polyak, I.; Reetz, M. T.; Thiel, W. *J. Am. Chem. Soc.* **2012**, *134*, 2732.
(32) Francl, M. M.; Pietro, W. J.; Hehre, W. J.; Binkley, J. S.; Gordon, M. S.; Defrees, D. J.; Pople, J. A. *J. Chem. Phys.* **1982**, *77*, 3654.
(33) Krishnan, R.; Binkley, J. S.; Seeger, R.; Pople, J. A. *J. Chem. Phys.* **1980**, *72*, 650.
(34) Frisch, M. J.; et al. *Gaussian 09*; Gaussian, Inc.: Wallingford, CT, 2009.
(35) Tian, B.; Strid, A.; Eriksson, L. A. *J. Phys. Chem. B* **2011**, *115*, 1918.

DOI: 10.1021/jo502651v
J. Org. Chem. 2015, 80, 2139−2147

(36) Badieyan, S.; Bevan, D. R.; Zhang, C. *Biochemistry* **2012**, *51*, 8907.
(37) Ball, S.; Bruice, T. C. *J. Am. Chem. Soc.* **1979**, *101*, 4017.
(38) Ball, S.; Bruice, T. C. *J. Am. Chem. Soc.* **1980**, *102*, 6498.
(39) Bruice, T. C.; Noar, J. B.; Ball, S. S.; Venkataram, U. V. *J. Am. Chem. Soc.* **1983**, *105*, 2452.
(40) Ottolina, G.; de Gonzalo, G.; Carrea, G. *J. Mol. Struct.: THEOCHEM* **2005**, *757*, 175.
(41) Bach, R. D.; Dmitrenko, O. *J. Phys. Chem. B* **2003**, *107*, 12851.
(42) Chaiyen, P.; Fraaije, M. W.; Mattevi, A. *Trends Biochem. Sci.* **2012**, *37*, 373.
(43) Massey, V. *J. Biol. Chem.* **1994**, *269*, 22459.
(44) Kemal, C.; Chan, T. W.; Bruice, R. C. *J. Am. Chem. Soc.* **1977**, *99*, 7272.
(45) Reed, A. E.; Curtiss, L. A.; Weinhold, F. *Chem. Rev.* **1988**, *88*, 899.
(46) Bach, R. D. *J. Phys. Chem. A* **2011**, *115*, 11087.
(47) Bach, R. D.; Dmitrenko, O. *J. Am. Chem. Soc.* **2006**, *128*, 1474.
(48) Ji, L.; Schuurmann, G. *Angew. Chem., Int. Ed.* **2013**, *52*, 744.
(49) Sucharitakul, J.; Tongsook, C.; Pakotiprapha, D.; van Berkel, W. J.; Chaiyen, P. *J. Biol. Chem.* **2013**, *288*, 35210.
(50) Crozier-Reabe, K. R.; Phillips, R. S.; Moran, G. R. *Biochemistry* **2008**, *47*, 12420.
(51) Kantz, A.; Gassner, G. T. *Biochemistry* **2011**, *50*, 523.
(52) Detmer, K.; Massey, V. *J. Biol. Chem.* **1984**, *259*, 11265.
(53) Taylor, M. G.; Massey, V. *J. Biol. Chem.* **1990**, *265*, 13687.
(54) Bach, R. D.; Mattevi, A. *J. Org. Chem.* **2013**, *78*, 8585.

DOI: 10.1021/jo502651v
J. Org. Chem. 2015, 80, 2139−2147